*American Mineralogist, Volume 91, pages 1249–1259, 2006*

# The arrojadite enigma: I. A new formula and a new model for the arrojadite structure

**FERNANDO CÁMARA,[1] ROBERTA OBERTI,[1,*] CHRISTIAN CHOPIN,[2] AND OLAF MEDENBACH[3]**

[1]CNR Istituto di Geoscienze e Georisorse (IGG), unità di Pavia, via Ferrata 1, I-27100 Pavia, Italy
[2]Laboratoire de Géologie, UMR 8538 du CNRS, Ecole normale supérieure, 24 rue Lhomond, F-75005 Paris, France
[3]Institut für Geologie, Mineralogie und Geophysik, Ruhr-Universität Bochum, 44780 Bochum, Germany

## ABSTRACT

A re-examination of the chemistry and structure of nearly all the known occurrences of arrojadite and related minerals (dickinsonite and sigismundite) allowed understanding of the main substitution vectors and cation ordering schemes ruling the crystal-chemistry of these very complex phosphates. Electron microprobe analyses were done with a careful choice of the standards and of experimental conditions, and were coupled with LA-ICP-MS in situ analysis for Li, Be, and B. Structure refinement was done in a space group (*Cc*) with a lower symmetry than those used in previous studies (*C*2/*c* and its equivalents), which allowed a better understanding of the structure details and of cation ordering. The combined approach yielded a new formula for the arrojadite group, namely $A_2B_2Ca_1Na_{2+x}M_{13}Al(PO_4)_{11}(PO_3OH_{1-x})W_2$, where A are either large divalent cations (Ba, Sr, Pb) plus vacancy, or monovalent (K, Na) cations; and B are either small divalent cations (Fe, Mn, Mg) plus vacancy, or monovalent (Na) cations. The number of hydroxyl groups in the arrojadite formula is generally 3 apfu, and can be lowered to 2 apfu in particular when the sum of non-(P,Al) cations is higher than 20 apfu.

We present in this paper the complete characterization of three samples (two of which are new members) that are crucial to fix the cornerstones of arrojadite crystal-chemistry. The sample from Rapid Creek (Yukon Territory) is the holotype for arrojadite-(KNa), and has unit formula $K_{0.83}Na_{5.01}(Ca_{0.91}Sr_{0.01})_{\Sigma=0.92}(Fe^{2+}_{9.34}Mg_{2.69}Mn^{2+}_{1.03}Zn_{0.01}Li_{0.01})_{\Sigma=13.08}(Al_{1.04}Ti_{0.02})_{\Sigma=1.06}(OH_{1.97}F_{0.03})_{\Sigma=2.00}[(P_{11.99}Si_{0.01}T_1)O_{47}(OH)_{1.00}]$ [ideally, $^{A1}K\,^{A2}Na\,^{B1}Na\,^{B2}Na\,^{Na1,2}Na_2\,^{Na3}\square\,^{Ca}Ca\,^{M}Fe_{13}Al(PO_4)_{11}\,^{P1x}(PO_3OH)\,^{W}(OH,F)_2$] and unit-cell dimensions: $a = 16.5220(11)$, $b = 10.0529(7)$, $c = 24.6477(16)$ Å, $\beta = 106.509(2)°$, $V = 3932.2(7)$ Å$^3$ ($Z = 4$). The sample from Horrsjöberg (Värmland, Sweden) is the holotype material for arrojadite-(SrFe), and has unit formula $Sr_{0.93}Na_{3.20}(Ca_{0.59}Ba_{0.20}Pb_{0.03}K_{0.03})_{\Sigma=0.85}(Fe^{2+}_{6.64}Mg_{3.61}Mn^{2+}_{3.33}Zn_{0.07}Li_{0.01})_{\Sigma=13.66}(Sc_{0.04}Al_{1.00})_{\Sigma=1.04}(OH_{1.10}F_{0.90})_{\Sigma=2.00}[(P_{11.95}Si_{0.02})_{\Sigma=11.97}O_{47}(OH)_{1.00}]$ [ideally, $^{A1}Sr\,^{A2}\square\,^{B1}Fe^{2+}\,^{B2}\square\,^{Na1,2}Na_2\,^{Na3}\square\,^{Ca}Ca\,^{M}Fe^{2+}_{13}Al(PO_4)_{11}\,^{P1x}(PO_3OH)\,^{W}(OH,F)_2$], and unit-cell dimensions $a = 16.3992(7)$, $b = 9.9400(4)$, $c = 24.4434(11)$ Å, $\beta = 105.489(1)°$, $V = 3839.76(46)$ Å$^3$. The sample from Branchville (Connecticut) is the holotype material for dickinsonite-(KMnNa), and has unit formula $K_{0.50}Na_{5.78}(Ca_{0.51}Sr_{0.05}Ba_{0.01}Pb_{0.01})_{\Sigma=0.58}(Mn^{2+}_{9.70}Fe^{2+}_{3.72}Li_{0.31}Mg_{0.06}Zn_{0.01})_{\Sigma=13.80}(Al_{0.91}Fe^{3+}_{0.09}Ti_{0.01})_{\Sigma=1.00}(OH_{1.97}F_{0.03})_{\Sigma=2.00}[(P_{12.02}Si_{0.01})_{\Sigma=12.03}O_{47}(OH)_{0.21}]$ [ideally, $^{A1}K\,^{A2}Na\,^{B1}Mn\,^{B2}\square\,^{Na1,2}Na_2\,^{Na3}Na\,^{Ca}Ca\,^{M}Mn_{13}Al(PO_4)_{11}\,^{P1x}(PO_4)\,^{W}(OH,F)_2$] and unit-cell dimensions $a = 16.6900(9)$, $b = 10.1013(5)$, $c = 24.8752(13)$ Å, $\beta = 105.616(2)°$, $V = 4038.9(7)$ Å$^3$.

**Keywords:** Crystal structure, arrojadite, analysis (chemical), new minerals, arrojadite-(KNa), arrojadite-(SrFe), dickinsonite-(KMnNa), optical properties, Raman spectroscopy, XRD data

## INTRODUCTION

"Arrojadites are infernally complex structures, with several partly occupied cations sites, and the complete details of their structures exceed our spatial parameters." This quotation is taken from Huminicki and Hawthorne (2002), page 186, in their review of known phosphate structures. In this pair of papers, we present the results of a general reconsideration of the known occurrences of arrojadite-group minerals (namely arrojadite, dickinsonite, and sigismundite), which is based on complete chemical analyses done with electron microprobe (EMP) and laser ablation-ICP-mass spectrometry (LA-ICP-MS), on single-crystal X-ray structure refinement (SREF), and on Raman spectroscopy.

This first paper focuses on a new model for the crystal structure of arrojadite, and on the crystallographic details that allowed us to fix the cornerstones of arrojadite crystal chemistry and thus, the basis for a new nomenclature scheme to be dealt with in Part II (Chopin et al. 2006, this volume).

The crystal structure of arrojadite was first determined in the *B*2/*b* space group on a sample from the Nickel Plate mine (Keystone, South Dakota) by Krutik et al. (1979), who did an isotropic refinement to $R = 14\%$ and proposed the formula $Na_1(Na, K, Ba, Sr)_1(Na, Ca)_2(Fe, Mn)_{10}Al(Li, Mg, Ca, Al, Fe, Mn)_4(PO_4)_8[PO_3(O, F, OH)]_4(OH)_2$ ($Z = 4$). The refined model has three independent sevenfold- to eightfold-coordinated sites occupied by large alkaline cations, one smaller octahedral site occupied by Al, seven independent fourfold- to sixfold-coordinated sites mainly occupied by Fe and Mn, six fourfold-coordinated sites occupied by P, and six OH groups per formula unit.

Merlino et al. (1981) did the anisotropic refinement ($R = 8\%$)

* E-mail: oberti@crystal.unipv.it

in the space group *C*2/*c* of another sample from the same locality, and proposed the ideal formula $KNa_4CaMn_4Fe_{10}Al(PO_4)_{12}(OH, F)_2$, where the number of sites suitable for large cations (X) was raised to five, and the number of OH groups was lowered to two. The new X1 site is disordered because its occupancy is incompatible with that of its centrosymmetric equivalent occurring at about 1 Å. The high displacement parameter observed at the P1 site was explained with a limited $(PO_4)^{3-} \leftrightarrow (OH)_4^{4-}$ exchange.

Moore et al. (1981) compared the refinement made by Merlino et al. (1981) with those made on a dickinsonite sample from Branchville, Connecticut, and on an arrojadite sample from Nancy Mine (North Groton, New Hampshire). The final *R* factor varies from 6 to 8%. Moore et al. (1981) chose the space group *A*2/*a*, and concluded that arrojadite and dickinsonite have the same structure and the general formula $[KNa_4Ca(Fe, Mn)_{14}^{2+}Al(OH)_2(PO_4)_{12}]$, with dickinsonite thus being the Mn-dominant analog of arrojadite. Compared to previous studies, they found evidence for a disordered P1x site, which complements the deficit at the P1 site previously pointed out by the high displacement parameter; the two phosphate groups share an *edge* of the basal face, but have vertices alternately pointing to opposite directions when seen along the *b* direction (Fig. 1). Two further disordered X sites were detected, which have ten- and twelve-fold coordination. With this , the arrojadite structure has 11 cationic and anionic sites confined to partial occupancy. The X1 site is at 0.5 Å from the inversion center, and thus is at most half occupied. Because they occur too close to each other, the occupancies of the X6, M1, P1, and P1x are mutually incompatible, as are those of the X4, X7, and P1x sites.

Demartin et al. (1996) investigated sigismundite, a Ba-dominant variety of arrojadite found at Madesimo (Spluga Valley, Italy), and proposed the simplified formula $(Ba, K, Pb)Na_3(Ca, Sr)(Fe, Mg, Mn)_{14}Al(OH)_2(PO_4)_{12}$. They did a weighted anisotropic structure refinement ($R = 7\%$) in the standard *C*2/*c* space group, but maintained the site nomenclature used by Moore et al. (1981). Barium was found to order at the X5 site, at a position slightly different from that of K; the X6 and X7 sites were found to be empty. A residue in the electron density map identified a new split site at 1 Å from the X4 site (X4x). Its occupancy is incompatible with those of the X4 and P1x sites. The steric relation between the P1 and P1x sites (P1 – P1x = 0.88 Å) was interpreted based on *face*-sharing tetrahedra, and was related to disorder at the adjacent M1 + M1x sites (M1 – M1x = 0.81 Å). A further structural difference from arrojadite is the coordination of the M7 site, which is an octahedron in sigismundite and a square pyramid in arrojadite.

Steele (2002) examined arrojadites from four localities, and found the space group *Cc* for the Rapid Creek (Yukon) and the Palermo mine (New Hampshire), and *C*2/*c* for the Chandler's Mills (New Hampshire) and the Nickel Plate mine (South Dakota). However, a unit formula $[AlCaKNa_5(Fe, Mn, Mg)_{13}(PO_4)_{12}F]$ provided in that abstract is not consistent with the *Cc* symmetry, and a second one for the *C*2/*c* specimens is not charge-balanced. Even if the intended meaning was $AlCaKNa_5(Fe, Mn, Mg)_{13}(PO_4)_{12}(OH)$ for *Cc* and $AlCaKNa_4(Fe, Mn, Mg)_{13}(PO_4)_{12}(F,OH)_2$ for *C*2/*c* specimens, the inconsistency persists and the occurrence of two different symmetries related to the exchange $Na_{-1}H_1$ remained unexplained.

There is no doubt that the structure and crystal chemistry of arrojadites, perhaps among the most complex found so far, need further investigation. The present work arose from the fortunate finding of an arrojadite-group mineral from Horrsjöberg (Värmland, Sweden) with a very peculiar composition, namely with high Sr and F contents coupled with an (Fe, Mn, Mg) content exceeding 13 atoms per formula unit (apfu). The quality of the collected diffraction data allowed us to understand that the symmetry could be lowered to *Cc*, yielding a model with 50 anionic sites, 12 sites suitable for P, one for Al, 13 sites suitable for transition metals, seven sites suitable for large alkaline cations, and three sites suitable for H. This model was successfully checked by complete chemical and structural investigation of a sample from Rapid Creek, Yukon Territory (Robinson et al. 1992) that has a composition very close to ideal arrojadite, and re-examination of a sample from Branchville, Connecticut; their

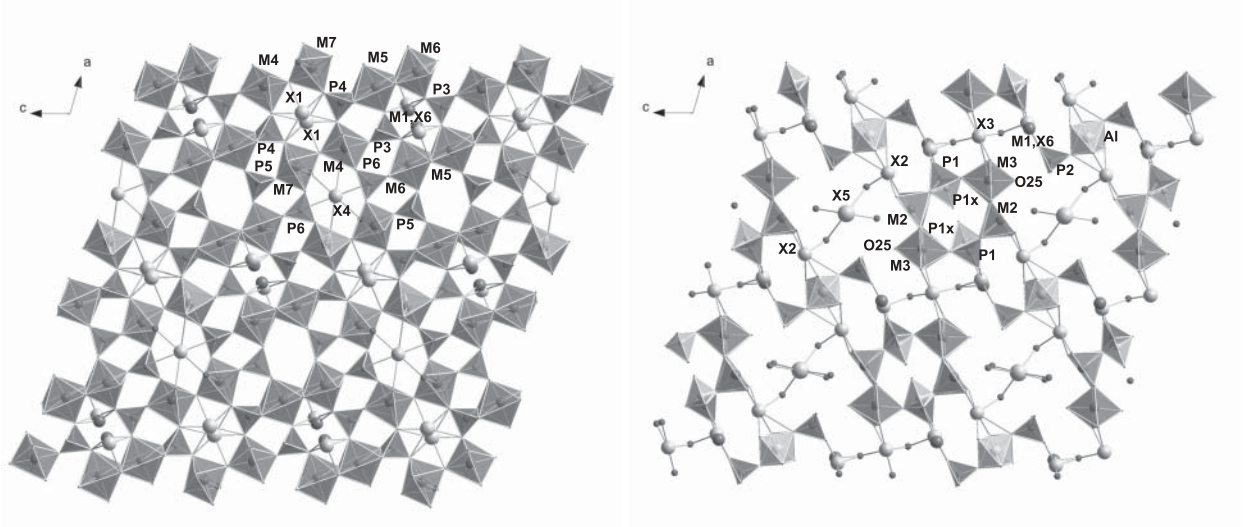


**FIGURE 1.** Projections onto (010) for the arrojadite structure refined in the *A*2/*a* space group (Moore et al. 1981): (**a**) the slab at y = ¼; (**b**) the slab at y = ½.

comparison allowed understanding of the main crystal-chemical mechanisms that are operative in the arrojadite group.

## EXPERIMENTAL METHODS

### Electron microprobe and LA-ICP-MS analysis

Electron-microprobe analyses were carried out in wavelength-dispersive mode with the Cameca SX50 instrument at Centre Camparis, Paris, at 15 kV, 15 nA beam current, 5–10 μm beam diameter, 10–15 s counting time on peak, using the PAP data-reduction program supplied by the manufacturer and the following standards: topaz (F*K*α), albite (Na*K*α), $Mg_3(PO_4)_2$ (Mg- and P*K*α), orthoclase (Al*K*α), diopside (Si- and Ca*K*α), $Sc_2O_3$ (Sc*K*α), $MnTiO_3$ (Ti- and Mn*K*α), hematite (Fe*K*α), sphalerite (Zn*K*α), $SrSiO_3$ (Sr*L*α), barite (Ba*L*α or -*L*β), and galena (Pb*L*α). Given the high Fe and Mn contents, EMP analysis of F was performed with the more dispersive TAP crystal rather than the W-Si multilayer PC1 crystal. Pulse-height analysis was used for analysis of F and P with the TAP crystal to eliminate contributions from the third-order P*K*α and second-order Ca*K*β lines. The use of Durango apatite as a P standard for the analysis of simple Mg, Fe, Mn-phosphates showed that the correct M:P stoichiometry is commonly not obtained to better than 1–2%. Therefore, regardless of other concerns raised against apatite (Stormer et al. 1993), we used synthetic $Mg_3(PO_4)_2$-III (Jaulmes et al. 1997) as a P and Mg standard and recommend use of similar anhydrous compounds in the case of complex phosphate stoichiometries.

A La-ICP-MS analysis was done because Li can be a common constituent of arrojadites. Also, the lower occupancies obtained by previous authors at the P1 site suggested that we check for the presence of small amounts of lower-Z tetrahedral cations, such as B and Be. Quantification of Li, Be, and B was done at the CNR-IGG (Pavia) with an instrument that couples a 266 nm Nd:YAG laser source (Brilliant-Quantel) to a quadrupole ICP-MS (DRCe - PerkinElmer). $^{6}$Li, $^{7}$Li, $^{9}$Be, $^{11}$B, $^{25}$Mg, $^{27}$Al, $^{29}$Si, and $^{43}$Ca were acquired in peak hopping mode with a dwell time of 10 ms. Each analysis involved the acquisition of 30 s of background and 1 min of signal. NIST610 and $^{29}$Al were adopted as external and internal standards, respectively. Data reduction was carried out with the Glitter software (van Achterbergh et al. 2001). Accuracy was tested on the BCR2 USGS reference glass and is estimated to be better than 5% relative.

Values of oxide wt% and unit formulae for the analysis of the refined crystals are reported in Table 1. Recalculation of the unit formulae was done on the basis of 47 O and 3 (OH, F) apfu for the samples from Horrsjöberg and Rapid Creek; for the sample from Branchville, the total number of (OH, F) apfu was calculated according to the content of the cationic sites, as explained in a following section.

### Single-crystal structure refinement

Crystals were hand-picked from mineral separates, and crystal quality was checked first from optical and then from diffraction behavior. Data collection was done with a Bruker/AXS SMART-Apex diffractometer at the CMR-IGG (Pavia). Ten batches of 900 images each (0.2° ω-rotation) were collected at different ϕ positions and at two different θ-arm positions (θ = 20°: 0, 90, 180, 270°; θ = 50°: 0, 45, 90, 135, 180, and 270°). The crystal-to-detector distance was 8 cm. Intensity data were integrated using the SAINT program (Bruker) and corrected for absorption using the SADABS program (Bruker). Structure refinement was done using a locally modified version of program ORFLS (Busing et al. 1962) with a model obtained starting from the coordinates of Moore et al. (1981) and allowing for the *Cc* symmetry. Selected crystal and refinement data are provided in Table 2.

Site nomenclature was changed to better address crystal-chemical exchanges and nomenclature issues. Details will be given in a companion paper (Chopin et al. 2006), where a table of conversion with respect to the previous reports will also be provided. In brief, the pairs of M and P sites no longer equivalent in the *Cc* symmetry maintain the number given by Moore et al. (1981), but assume the a and b suffixes. The P1 and P1x sites are no longer partially superimposed, and have full occupancy. The X sites have been completely renamed to account for the observed heterovalent exchanges.

Atomic coordinates, displacement parameters, and refined site-scattering values are reported in Table 3. Interatomic distances for the P sites (Table 4a), the Al and M sites (Table 4b), and the alkali sites (Tables 4c and 4d) are reported in Table 4. Lists of measured structure factors have also been deposited as Table 5[1].

[1] Deposit item AM-06-021, Tables 3 and 5. Deposit items are available two ways: For a paper copy contact the Business Office of the Mineralogical Society of America (see inside front cover of recent issue) for price information. For an electronic copy visit the MSA web site at http://www.minsocam.org, go to the American Mineralogist Contents, find the table of contents for the specific volume/issue wanted, and then click on the deposit link there.

**TABLE 1.** Chemical analysis (EMP + LA-ICP-MS); unit formulae recalculated based on 47 O and 3 (OH, F) pfu for the samples from Rapid Creek and Horrsjöberg, and on 47 O and (3 – Na3) (OH, F) pfu for the sample from Branchville

| Oxide wt% | Rapid Creek | Horrsjöberg | Branchville |
|---|---|---|---|
| Mean of | 6 | 11 | 7 |
| $P_2O_5$ | 41.20(11) | 40.74(32) | 39.01(25) |
| $SiO_2$ | 0.01(1) | 0.06(4) | 0.01(1) |
| $TiO_2$ | 0.07(2) | 0.01(2) | 0.02(3) |
| $Al_2O_3$ | 2.56(9) | 2.46(9) | 2.12(4) |
| MgO | 5.23(1) | 7.00(38) | 0.08(1) |
| $FeO_{total}$ | 32.40(70) | 22.94(22) | 12.52(41) |
| MnO | 3.54(17) | 11.34(60) | 31.47(17) |
| ZnO | 0.04(5) | 0.28(6) | 0.02(4) |
| CaO | 2.48(7) | 1.58(23) | 1.31(16) |
| SrO | 0.03(3) | 4.63(68) | 0.25(6) |
| BaO | 0.02(6) | 1.48(93) | 0.04(4) |
| PbO | 0.03(3) | 0.29(13) | 0.09(8) |
| $Na_2O$ | 7.50(10) | 4.77(12) | 8.19(10) |
| $K_2O$ | 1.90(6) | 0.06(3) | 1.07(9) |
| $Li_2O$ * | 0.005 | 0.006 | 0.213 |
| F | 0.02(2) | 0.82(12) | 0.02(4) |
| O=F | 0.01 | 0.35 | 0.01 |
| $H_2O_{calc}$ | 1.31 | 0.91 | 0.90 |
| sum | 98.35 | 99.17 | 97.33 |
| | | | |
| P | 11.99 | 11.95 | 12.02 |
| Si | 0.01 | 0.02 | 0.01 |
| Ti | 0.02 | 0.01 | 0.01 |
| Al | 1.04 | 1.00 | 0.91 |
| Mg | 2.69 | 3.61 | 0.06 |
| $Fe^{2+}$ | 9.34 | 6.64 | 3.72 |
| $Fe^{3+}$ | | | 0.09 |
| Mn | 1.03 | 3.33 | 9.70 |
| Zn | 0.01 | 0.07 | 0.01 |
| Ca | 0.91 | 0.59 | 0.51 |
| Sr | 0.01 | 0.93 | 0.05 |
| Ba | 0.00 | 0.20 | 0.01 |
| Pb | 0.00 | 0.03 | 0.01 |
| Na | 5.01 | 3.20 | 5.78 |
| K | 0.83 | 0.03 | 0.50 |
| Li | 0.01 | 0.006 | 0.31 |
| F | 0.03 | 0.90 | 0.03 |
| $H_{calc}$ | 2.97 | 2.10 | 2.18 |
| | | | |
| cat sum ‡ | 19.84 | 18.64 | 20.66 |
| ΣM-type | 13.08 | 13.66 | 13.80 |
| ΣX-type | 6.76 | 4.98 | 6.86 |
| | | | |
| s.s. $M_{calc}$§ | 299.2 | 283.8 | 320.5 |
| s.s. $M_{obs}$ | 302.0 | 280.7 | 321.5 |
| s.s. $X_{calc}$ | 92.2 | 115.8 | 106.7 |
| s.s. $X_{obs}$ | 94.3 | 111.2 | 99.6 |
| s.s. $tot_{calc}$ | 391.4 | 399.7 | 427.2 |
| s.s. $tot_{obs}$ | 396.3 | 391.9 | 421.1 |
| Δtot (%) | 1.2 | 2.0 | 1.5 |

* $Li_2O$ measured in situ by LA-ICP-MS (3 point analyses; estimated accuracy ±5%); B = 0.7 ppm and 1.3 ppm, and Be = 1 ppm and 2.8 ppm for Rapid Creek and Branchville, respectively.
‡ Sum of the cations beyond P + Si + Al + H.
§ s.s. = site scattering calculated from chemical analyses (calc) and obtained by structure refinement (obs).

### Raman spectroscopy

Reconnaissance Raman spectra were obtained in the OH-stretching region on unoriented crystal fragments with a Renishaw inVia microspectrometer at ENS (Paris), using a 514 nm laser in polarized mode delivering 2 to 5 mW on the sample, a long-working-distance ×50 objective lens with 0.5 numerical aperture, and 1800 grooves/mm gratings. Spectral deconvolution was made with a Voigt function, imposing the same FWHM for all component bands of a given spectrum.

## Results and discussion

### A new model for the arrojadite structure

The present work shows that the correct space group of arrojadite structure is *Cc*. The basic features of the structure are those discussed by Moore et al. (1981). In fact, the lowering of the symmetry does not change the framework built up by the P tetrahedra and the M polyhedra, but simply avoids both the partial superposition of the P1 and P1x tetrahedra and the close contacts between cationic sites discussed above; it also cancels out the centrosymmetric analog of the X1 site (Ca in the new nomenclature). All the 86 sites present in the *Cc* model can be fully occupied, and the only crystallographic constraint is the inverse relation between the occupancies of the Na3 and the H3x sites, which will be discussed in detail in the following section. The new model of the arrojadite structure is shown in Figure 2.

The lowering in symmetry yields a significant lowering of the *R* factors, and calculation of difference Fourier maps after convergence shows that the more intense residual peaks are related to the bonding feature at the M and P sites. Within the pairs of M sites that are no longer equivalent in the *Cc* symmetry (now denoted by a and b), there are significant differences both in terms of refined bond-lengths and site-scattering values (cf. Tables 2 and 3). This feature also implies the existence of significant cation ordering; ordering patterns will be discussed in a future contribution, where the available chemical, structural, and spectroscopic information on all the examined arrojadite samples will be compared and discussed.

However, a conclusion drawn from Raman analysis is relevant to the present discussion. In fact, all the 12 samples examined (among which those from Chandler's Mills and the Nickel Plate mine that had been described in the centrosymmetric space group by Merlino et al. 1981 and Steele 2002) show two distinct clusters of bands in the OH-stretching region (Fig. 3) that can be related to H atoms occurring at the two independent W1 and W2 sites (which would merge into a unique W site in the *C*2/*c* space group). The number of the bands observed in each cluster depends on the chemistry of the M sites, and the relative intensity of the two clusters confirms that F tends to order at the W1 site, as shown by the structure refinement (cf. the Yukon and Horrsjöberg spectra, and see the next section for more detail). In any event, the presence of the two clusters in all spectra is clear evidence that *Cc* is the true space group for all arrojadites. The fact that some samples still show some "ghost" residual electron density maxima similar to those previously reported by Moore et al. (1981) is probably due to some microstructural effects (for instance, domains related by rotation of 180° around **b** and a **c**/2 glide), which are presently investigated by HRTEM.

**Table 2.** Selected crystal and refinement data for the studied arrojadites

| Locality | Rapid Creek | Horrsjöberg | Branchville |
|---|---|---|---|
| museum code | 41081 | 16926 | 4861 |
| IGG code* | *isd* | *iri* | *itb* |
| system | Monoclinic | Monoclinic | Monoclinic |
| space group | *Cc* | *Cc* | *Cc* |
| *a* (Å) | 16.5520(11) | 16.3992(7) | 16.6900(9) |
| *b* (Å) | 10.0529(7) | 9.9400(4) | 10.1013(5) |
| *c* (Å) | 24.6477(16) | 24.4434(11) | 24.8752(13) |
| β (°) | 106.509(2) | 105.489(1) | 105.616(2) |
| Volume (Å³) | 3932.2(7) | 3839.8(3) | 4038.9(7) |
| *Z* | 4 | 4 | 4 |
| θ range | 1.7–35.0° | 1.7–35.0° | 1.7–35.0° |
| no. coll. refl.† | 27444 | 26719 | 27997 |
| <redundancy> | 3.03 | 3.02 | 3.00 |
| no. unique refl. | 8656 | 8447 | 8898 |
| *R*(int) (%) | 2.75 | 2.30 | 4.80 |
| I/σI cut | 3 | 3 | 3 |
| no. obs | 7953 | 7987 | 8381 |
| no. refined par. | 847 | 842 | 862 |
| *R* obs (%) | 2.88 | 3.95 | 3.85 |
| *R* all (%) | 3.25 | 4.45 | 4.09 |

* This symbol identifies the sample in the archives.
† Number of collected reflections, after averaging those collected more than once.

**Table 4a.** The phosphate groups: Interatomic distances (Å) and selected geometrical parameters for the arrojadites of this work

| | Rapid Creek | Horrsjöberg | Branchville | | Rapid Creek | Horrsjöberg | Branchville | | Rapid Creek | Horrsjöberg | Branchville |
|---|---|---|---|---|---|---|---|---|---|---|---|
| P1-O1b | 1.549 (3) | 1.533 (3) | 1.546 (4) | P1x-O1a | 1.527 (3) | 1.532 (3) | 1.538 (4) | P2a-O5a | 1.558 (3) | 1.552 (3) | 1.548 (4) |
| P1-O2b | 1.536 (3) | 1.531 (3) | 1.542 (4) | P1x-O2a | 1.523 (3) | 1.539 (3) | 1.539 (4) | P2a-O6a | 1.524 (4) | 1.524 (4) | 1.521 (5) |
| P1-O3 | 1.519 (3) | 1.533 (3) | 1.532 (4) | P1x-O3x | 1.581 (3) | 1.559 (3) | 1.525 (7) | P2a-O7a | 1.559 (4) | 1.555 (4) | 1.550 (5) |
| P1-O4 | 1.535 (3) | 1.542 (3) | 1.529 (4) | P1x-O4x | 1.516 (1) | 1.518 (1) | 1.511 (4) | P2a-O8a | 1.512 (4) | 1.528 (4) | 1.519 (4) |
| mean | 1.535 | 1.535 | 1.537 | mean | 1.537 | 1.537 | 1.528 | mean | 1.538 | 1.539 | 1.535 |
| *V* (Å³) | 1.85 | 1.85 | 1.86 | *V* (Å³) | 1.86 | 1.86 | 1.83 | *V* (Å³) | 1.85 | 1.86 | 1.84 |
| TAV | 3.69 | 6.06 | 1.78 | TAV | 11.61 | 9.23 | 8.02 | TAV | 21.99 | 23.56 | 19.14 |
| TQE | 1.0010 | 1.0015 | 1.0005 | TQE | 1.0030 | 1.0024 | 1.0022 | TQE | 1.0055 | 1.0058 | 1.0048 |
| P3a-O9a | 1.535 (3) | 1.529 (3) | 1.527 (4) | P3b-O9b | 1.533 (3) | 1.534 (3) | 1.533 (4) | P4a-O13a | 1.552 (3) | 1.547 (3) | 1.544 (4) |
| P3a-O10a | 1.522 (3) | 1.528 (3) | 1.526 (5) | P3b-O10b | 1.537 (3) | 1.530 (3) | 1.532 (5) | P4a-O14a | 1.539 (3) | 1.539 (3) | 1.537 (4) |
| P3a-O11a | 1.553 (3) | 1.553 (3) | 1.546 (5) | P3b-O11b | 1.524 (3) | 1.516 (3) | 1.511 (4) | P4a-O15a | 1.537 (3) | 1.533 (3) | 1.526 (4) |
| P3a-O12a | 1.523 (3) | 1.537 (3) | 1.537 (4) | P3b-O12b | 1.558 (3) | 1.550 (3) | 1.547 (4) | P4a-O16a | 1.527 (3) | 1.523 (3) | 1.517 (4) |
| mean | 1.533 | 1.537 | 1.534 | mean | 1.538 | 1.533 | 1.531 | mean | 1.539 | 1.535 | 1.531 |
| *V* (Å³) | 1.85 | 1.86 | 1.85 | *V* (Å³) | 1.87 | 1.85 | 1.84 | *V* (Å³) | 1.86 | 1.85 | 1.83 |
| TAV | 4.12 | 5.15 | 6.78 | TAV | 2.62 | 4.56 | 2.99 | TAV | 14.74 | 13.98 | 15.90 |
| TQE | 1.0011 | 1.0013 | 1.0017 | TQE | 1.0006 | 1.0011 | 1.0008 | TQE | 1.0037 | 1.0035 | 1.0040 |
| P5a-O17a | 1.523 (3) | 1.528 (3) | 1.525 (5) | P5b-O17b | 1.528 (3) | 1.531 (3) | 1.532 (4) | P6a-O21a | 1.527 (4) | 1.529 (4) | 1.523 (5) |
| P5a-O18a | 1.513 (3) | 1.528 (3) | 1.513 (5) | P5b-O18b | 1.513 (3) | 1.524 (3) | 1.524 (4) | P6a-O22a | 1.511 (4) | 1.525 (4) | 1.513 (5) |
| P5a-O19a | 1.541 (4) | 1.544 (4) | 1.540 (5) | P5b-O19b | 1.549 (3) | 1.543 (3) | 1.544 (5) | P6a-O23a | 1.544 (4) | 1.534 (4) | 1.543 (5) |
| P5a-O20a | 1.550 (3) | 1.538 (3) | 1.533 (4) | P5b-O20b | 1.548 (3) | 1.558 (3) | 1.550 (4) | P6a-O24a | 1.544 (4) | 1.554 (4) | 1.555 (5) |
| mean | 1.532 | 1.535 | 1.528 | mean | 1.535 | 1.539 | 1.537 | mean | 1.531 | 1.535 | 1.533 |
| *V* (Å³) | 1.84 | 1.85 | 1.83 | *V* (Å³) | 1.85 | 1.87 | 1.86 | *V* (Å³) | 1.84 | 1.86 | 1.85 |
| TAV | 2.59 | 4.76 | 3.14 | TAV | 1.76 | 6.55 | 0.94 | TAV | 1.84 | 3.70 | 1.77 |
| TQE | 1.0007 | 1.0013 | 1.0008 | TQE | 1.0006 | 1.0017 | 1.0003 | TQE | 1.0006 | 1.0010 | 1.0005 |

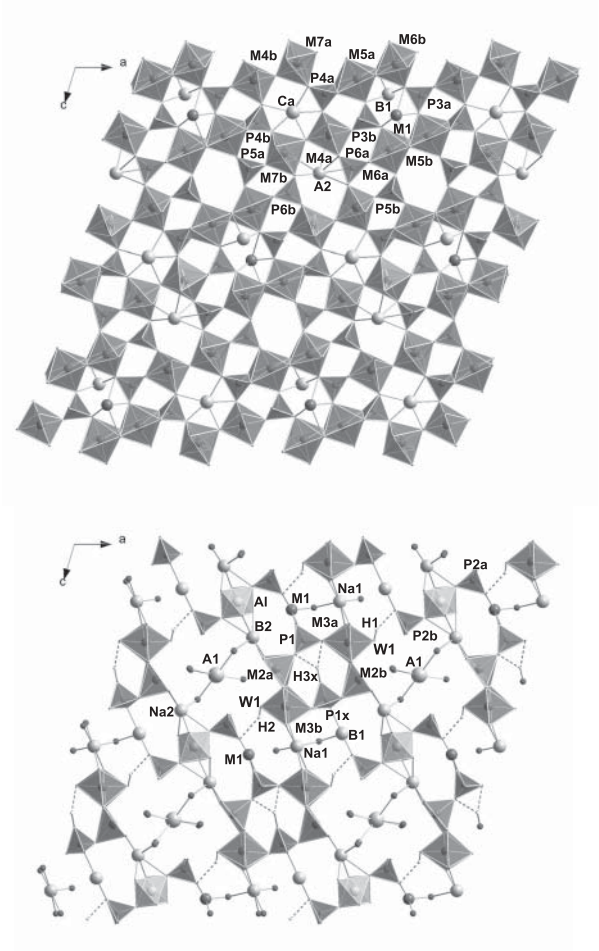


**FIGURE 2.** Projections onto (010) for the arrojadite structure refined in the *Cc* space group (this work): (**a**) the slab at y = ¼; (**b**) the slab at y = ½.

**TABLE 4A**—*Extended*

| | Rapid Creek | Horrsjöberg | Branchville |
|---|---|---|---|
| P2b-O5b | 1.546 (3) | 1.544 (3) | 1.551 (4) |
| P2b-O6b | 1.520 (3) | 1.514 (3) | 1.520 (5) |
| P2b-O7b | 1.530 (3) | 1.532 (3) | 1.536 (5) |
| P2b-O8b | 1.538 (3) | 1.526 (3) | 1.526 (4) |
| mean | 1.533 | 1.529 | 1.533 |
| *V* (Å³) | 1.84 | 1.83 | 1.84 |
| TAV | 18.33 | 14.14 | 11.32 |
| TQE | 1.0047 | 1.0036 | 1.0028 |
| P4b-O13b | 1.555 (3) | 1.557 (3) | 1.561 (4) |
| P4b-O14b | 1.540 (3) | 1.536 (3) | 1.539 (4) |
| P4b-O15b | 1.525 (3) | 1.521 (3) | 1.520 (4) |
| P4b-O16b | 1.525 (3) | 1.526 (3) | 1.532 (4) |
| mean | 1.536 | 1.535 | 1.538 |
| *V* (Å³) | 1.85 | 1.85 | 1.86 |
| TAV | 14.95 | 16.06 | 15.16 |
| TQE | 1.0037 | 1.0040 | 1.0038 |
| P6b-O21b | 1.527 (4) | 1.527 (4) | 1.532 (4) |
| P6b-O22b | 1.530 (4) | 1.532 (4) | 1.516 (5) |
| P6b-O23b | 1.546 (4) | 1.534 (4) | 1.537 (5) |
| P6b-O24b | 1.552 (4) | 1.563 (4) | 1.550 (5) |
| mean | 1.539 | 1.539 | 1.534 |
| *V* (Å³) | 1.87 | 1.87 | 1.85 |
| TAV | 0.89 | 6.04 | 0.89 |
| TQE | 1.0003 | 1.0016 | 1.0003 |

## The correct number of OH groups, and evidence for F site preference

Three H atoms could be located in a straightforward manner in the difference Fourier maps of the samples from Rapid Creek. Two of them, H1 and H2, are bonded to the W1 and W2 sites, which are coordinated to the M3a and M3b octahedra, respectively. Both the H1 and H2 atoms are involved in a hydrogen bond with the O8b and O8a oxygen atoms, respectively (Fig. 4a).

The third H atom (H3x) is bonded to O3x, the apical oxygen atom of the new P1x tetrahedron, and occurs in a position close to that of the Na3 site, which is analogous to the X7 site in Moore et al. (1981); therefore, the presence of the third proton is incompatible with Na3 occupancy (Fig. 4b). The H3x hydrogen is involved in a bifurcated hydrogen bond with the O3 (at 2.47 Å) and the O1b (at 2.53 Å) oxygen atoms.

In the sample from Horrsjöberg, the electron-density maximum corresponding to the H1 atom was hardly detectable, in agreement with the preferential order of F at the W1 site shown by the refined site-scattering value at W1 and the short M3a-W1 distance. In the sample from Branchville, where the Na3 site occupancy is almost complete, there is almost no indication for the presence of a maximum suitable for H3x (Fig. 5).

These pieces of evidence were validated by bond valence analysis (using the values reported by Brown and Altermatt 1985) based on refined bond lengths and site assignment. In

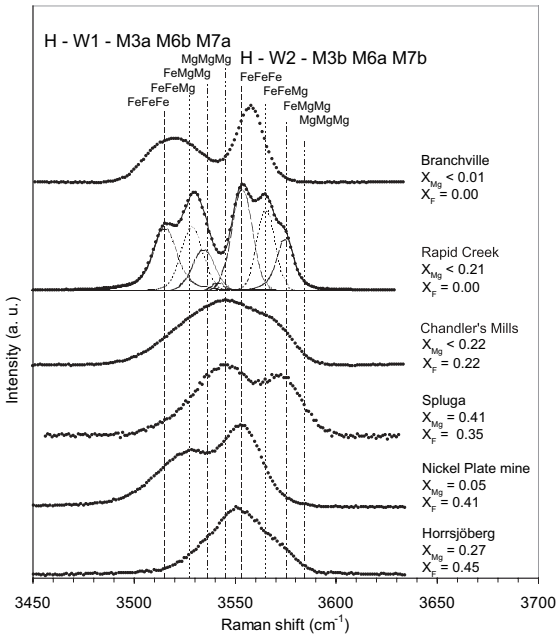


**FIGURE 3.** Raman spectra (OH-stretching region) of dickinsonite and arrojadite samples arranged in order of increasing fluorine contents. $X_F$ = F/(F + $^{W}$OH), $X_{Mg}$ = Mg/(Mg + Fe + Mn + Zn). Note the two clusters of bands, which demonstrate that the non-centrosymmetric space group *Cc* is correct for all the samples. The low-wavenumber cluster is quite weak in Horrsjöberg, suggesting that F is preferentially incorporated at this site. A deconvolution of the Rapid Creek spectrum shows the contribution of various local M3a-M6b-M7a and M3b-M6a-M7b environments around the W1 and W2 sites, respectively.

**TABLE 4B.** The Al and M sites: Interatomic distances (Å) and selected geometrical parameters for the arrojadites of this work

| | Rapid Creek | Horrsjöberg | Branchville | | Rapid Creek | Horrsjöberg | Branchville | | Rapid Creek | Horrsjöberg | Branchville |
|---|---|---|---|---|---|---|---|---|---|---|---|
| Al-O5a | 1.860 (2) | 1.868 (3) | 1.885 (4) | M1-O4 | 2.020 (3) | 2.034 (3) | 2.094 (4) | M2a-O4x | 2.164 (3) | 2.226 (3) | 2.246 (4) |
| Al-O5b | 1.866 (2) | 1.855 (3) | 1.885 (4) | M1-O8b | 2.016 (3) | 2.043 (3) | 2.070 (4) | M2a-O19a | 2.135 (3) | 2.150 (3) | 2.134 (4) |
| Al-O10a | 1.901 (2) | 1.892 (3) | 1.919 (4) | M1-O11a | 2.021 (3) | 2.072 (3) | 2.120 (4) | M2a-O20b | 2.139 (3) | 2.118 (4) | 2.172 (4) |
| Al-O10b | 1.894 (2) | 1.890 (3) | 1.918 (4) | M1-O12a | 2.746 (3) | 2.386 (4) | 2.438 (5) | M2a-O23a | 2.036 (3) | 2.080 (3) | 2.103 (4) |
| Al-O13a | 1.889 (2) | 1.878 (3) | 1.894 (4) | M1-O12b | 2.022 (3) | 2.008 (3) | 2.062 (4) | M2a-O24b | 2.012 (3) | 2.122 (3) | 2.173 (5) |
| Al-O13b | 1.891 (2) | 1.888 (3) | 1.903 (4) | mean$^{IV}$ | 2.020 | 2.039 | 2.086 | mean | 2.097 | 2.139 | 2.165 |
| mean | 1.883 | 1.878 | 1.900 | V$^{IV}$ (Å$^3$) | 3.85 | 3.73 | 4.06 | *V* (Å$^3$) | 6.66 | 6.63 | 7.33 |
| *V* (Å$^3$) | 8.89 | 8.82 | 9.13 | mean$^{V}$ | 2.165 | 2.108 | 2.157 | | | | |
| OAV | 5.61 | 5.05 | 5.27 | V$^{V}$ (Å$^3$) | 7.55 | 7.46 | 7.89 | | | | |
| OQE | 1.0017 | 1.0015 | 1.0015 | | | | | | | | |
| M3a-O1a | 2.232 (3) | 2.143 (3) | 2.225 (4) | M3b-O1b | 2.203 (3) | 2.163 (3) | 2.268 (4) | M4a-O1b | 2.117 (2) | 2.054 (3) | 2.130 (4) |
| M3a-O9a | 2.164 (3) | 2.112 (3) | 2.256 (4) | M3b-O9b | 2.134 (3) | 2.132 (3) | 2.175 (4) | M4a-O5a | 2.191 (2) | 2.148 (3) | 2.194 (4) |
| M3a-O14a | 2.029 (3) | 1.999 (3) | 2.082 (4) | M3b-O14b | 2.060 (3) | 2.009 (3) | 2.065 (4) | M4a-O7a | 2.157 (2) | 2.116 (3) | 2.180 (4) |
| M3a-O19b | 2.177 (3) | 2.120 (4) | 2.194 (4) | M3b-O19a | 2.090 (3) | 2.140 (3) | 2.181 (5) | M4a-O9b | 2.099 (2) | 2.081 (3) | 2.125 (4) |
| M3a-O23b | 2.013 (3) | 2.025 (3) | 2.067 (4) | M3b-O23a | 2.083 (3) | 2.045 (3) | 2.118 (5) | M4a-O15a | 2.140 (2) | 2.308 (3) | 2.206 (4) |
| M3a-W1 | 2.065 (3) | 2.020 (3) | 2.116 (4) | M3b-W2 | 2.077 (3) | 2.066 (3) | 2.134 (4) | M4a-O21a | 2.061 (3) | 2.052 (3) | 2.119 (5) |
| mean | 2.1130 | 2.0700 | 2.157 | mean | 2.108 | 2.092 | 2.157 | mean | 2.128 | 2.127 | 2.159 |
| *V* (Å$^3$) | 12.35 | 11.64 | 13.11 | *V* (Å$^3$) | 12.27 | 11.95 | 13.04 | *V* (Å$^3$) | 12.26 | 12.16 | 12.76 |
| OAV | 39.99 | 34.19 | 45.78 | OAV | 42.22 | 51.40 | 59.85 | OAV | 105.03 | 118.64 | 114.31 |
| OQE | 1.0139 | 1.0108 | 1.0148 | OQE | 1.0126 | 1.0155 | 1.0182 | OQE | 1.0319 | 1.0378 | 1.0346 |
| M5a-O2a | 2.130 (2) | 2.132 (3) | 2.121 (5) | M5b-O2b | 2.113 (3) | 2.136 (3) | 2.175 (4) | M6a-O2b | 2.271 (2) | 2.249 (3) | 2.332 (4) |
| M5a-O6b | 2.093 (2) | 2.112 (3) | 2.130 (4) | M5b-O6a | 2.125 (3) | 2.109 (3) | 2.133 (4) | M6a-O6a | 2.129 (3) | 2.146 (3) | 2.203 (4) |
| M5a-O11b | 2.093 (2) | 2.087 (3) | 2.113 (4) | M5b-O11a | 2.144 (3) | 2.128 (3) | 2.093 (5) | M6a-O12b | 2.143 (3) | 2.175 (3) | 2.225 (4) |
| M5a-O13a | 2.313 (2) | 2.296 (3) | 2.355 (4) | M5b-O13b | 2.270 (3) | 2.279 (3) | 2.320 (4) | M6a-O18b | 1.997 (3) | 2.071 (3) | 2.120 (5) |
| M5a-O14a | 2.252 (2) | 2.243 (3) | 2.227 (4) | M5b-O14b | 2.254 (3) | 2.239 (3) | 2.276 (4) | M6a-O24a | 2.605 (4) | 2.359 (4) | 2.282 (5) |
| M5a-O17b | 2.004 (2) | 2.017 (3) | 2.034 (4) | M5b-O17a | 2.012 (3) | 2.037 (3) | 2.052 (4) | M6a-W2 | 2.234 (3) | 2.252 (3) | 2.202 (4) |
| mean | 2.148 | 2.148 | 2.163 | mean | 2.153 | 2.155 | 2.175 | mean | 2.230 | 2.209 | 2.227 |
| *V* (Å$^3$) | 12.35 | 12.36 | 12.55 | *V* (Å$^3$) | 12.48 | 12.52 | 12.86 | *V* (Å$^3$) | 14.22 | 13.96 | 14.17 |
| OAV | 150.10 | 149.54 | 162.74 | OAV | 145.73 | 143.33 | 144.31 | OAV | 84.65 | 65.02 | 91.42 |
| OQE | 1.0483 | 1.0477 | 1.0522 | OQE | 1.0456 | 1.0445 | 1.0460 | OQE | 1.0337 | 1.0209 | 1.0271 |
| M7a-O4x | 2.344 (2) | 2.258 (3) | 2.310 (4) | M7b-O3 | 2.659 (3) | 2.350 (3) | 2.596 (5) | | | | |
| M7a-O7b | 2.082 (2) | 2.044 (3) | 2.139 (4) | M7b-O7a | 2.130 (3) | 2.095 (3) | 2.191 (4) | | | | |
| M7a-O16a | 2.169 (2) | 2.130 (4) | 2.199 (4) | M7b-O16b | 2.145 (3) | 2.211 (3) | 2.190 (4) | | | | |
| M7a-O20b | 2.104 (2) | 2.102 (3) | 2.233 (4) | M7b-O20a | 2.146 (3) | 2.175 (3) | 2.288 (5) | | | | |
| M7a-O22a | 2.035 (3) | 2.034 (3) | 2.109 (5) | M7b-O22b | 2.067 (3) | 2.086 (4) | 2.101 (4) | | | | |
| M7a-W1 | 2.214 (3) | 2.181 (4) | 2.270 (4) | M7b-W2 | 2.173 (3) | 2.222 (3) | 2.205 (5) | | | | |
| mean | 2.158 | 2.125 | 2.210 | mean | 2.220 | 2.190 | 2.262 | | | | |
| V (Å$^3$) | 13.00 | 12.48 | 13.74 | *V* (Å$^3$) | 13.63 | 13.45 | 14.40 | | | | |
| OAV | 66.51 | 54.94 | 103.86 | OAV | 142.10 | 87.88 | 150.94 | | | | |
| OQE | 1.0228 | 1.0179 | 1.0323 | OQE | 1.0548 | 1.0287 | 1.0522 | | | | |

the sample from Yukon, where the A2 site is fully occupied by Na, the bond valence incident to O3x is 1.30 v.u.; in the sample from Horrsjöberg, the bond valence incident to O3x is 1.16 v.u. when A2 is locally vacant and 1.36 if A2 is locally occupied by Na; in the sample from Branchville, the bond valence incident to O3x is 1.28 v.u. when A2 is locally vacant, 1.50 when A2 is locally occupied by Na, and 1.98 when both A2 and Na3 are locally occupied by Na.

The occurrence of the third proton could not be noticed by Moore et al. (1981) in the *C*2/*c* model, where the region around the P1 and P1x tetrahedra is affected mostly by widespread superposition of sites.

Among all the samples we have examined, only those from Branchville and from the Nickel Plate Mine have significant Na3 site occupancy. In their case, the total number of H atoms per formula unit must be calculated as 3 – Na3. When the occupancy of the Na3 site is unknown, crystal-chemical arguments given in detail in Part II (Chopin et al. 2006. this volume) support the use of the relation OH + F = 2 + [21 – the sum of non-(P,Al) cations] for the recalculation of the unit formula.

The amount of F in arrojadites rarely exceeds 1.0 apfu, and we never found evidence for its occurrence at the O3x site, which fixes the maximum F content in arrojadite at 2.0 apfu. Refined site-scattering values and bond lengths suggest that F has a strong preference for the W1 site.

## Cation ordering

The arrojadite structure is very conservative with regard to the charge arrangement. At the P tetrahedra, the Si content is always very low (<0.05 apfu), and the B and Be contents are nil or negligible. The Al site is always occupied by trivalent cations: Al and Sc for the samples of this work, $Fe^{3+}$ in sample from Branchville and in some analyses in the literature (Robinson et al. 1992) and in the synthetic phase of Yakubovich et al. (1986). The M sites are always occupied by divalent cations (Fe, Mn, Mg, Zn), with the only exception being Li.

Given the good agreement between the refined site-scattering values and those calculated from the unit formulae (Table 1), some conclusions could be drawn about the site preference of most cations.

At the M sites, both the refined site-scattering values and bond lengths suggest that Mg is incorporated preferentially at the M3 (a and b), M4b, and M2b sites (cf. the samples from Rapid Creek and Horrsjöberg). Comparative crystal-chemical analysis generally shows that Li is always an M-type cation (cf. also Part II, Chopin et al. 2006, this volume); however, it usually distributes among many sites, with a preference for M1 (cf. the low site-scattering value obtained for the sample from Branchville, where the Li content reaches 0.30 apfu).

The most important implication of the present work is the recognition of the number, the coordination, and the crystal-

**TABLE 4B**—*Extended*

| | Rapid Creek | Horrsjöberg | Branchville |
|---|---|---|---|
| M2b-O3 | 2.044 (3) | 2.025 (3) | 2.112 (4) |
| M2b-O19b | 2.072 (3) | 2.080 (3) | 2.113 (4) |
| M2b-O20a | 2.081 (3) | 2.131 (4) | 2.108 (5) |
| M2b-O23b | 2.105 (3) | 2.097 (3) | 2.159 (4) |
| M2b-O24a | 2.066 (3) | 2.095 (3) | 2.179 (5) |
| mean | 2.074 | 2.085 | 2.134 |
| *V* (Å³) | 6.54 | 6.48 | 6.89 |
| M4b-O1a | 2.056 (3) | 2.032 (3) | 2.074 (5) |
| M4b-O5b | 2.202 (3) | 2.160 (3) | 2.249 (5) |
| M4b-O7b | 2.106 (3) | 2.107 (3) | 2.168 (5) |
| M4b-O9a | 2.140 (3) | 2.116 (3) | 2.147 (4) |
| M4b-O15b | 2.173 (3) | 2.177 (3) | 2.232 (5) |
| M4b-O21b | 2.034 (3) | 2.075 (3) | 2.108 (4) |
| mean | 2.119 | 2.111 | 2.163 |
| *V* (Å³) | 12.07 | 11.92 | 12.81 |
| OAV | 112.07 | 114.66 | 116.72 |
| OQE | 1.0344 | 1.0354 | 1.0365 |
| M6b-O2a | 2.368 (3) | 2.317 (3) | 2.370 (4) |
| M6b-O6b | 2.131 (3) | 2.144 (3) | 2.207 (4) |
| M6b-O12a | 2.079 (3) | 2.157 (3) | 2.218 (4) |
| M6b-O18a | 1.954 (3) | 2.032 (3) | 2.068 (5) |
| M6b-O24b | 2.733 (4) | 2.335 (4) | 2.304 (4) |
| M6b-W1 | 2.220 (3) | 2.280 (3) | 2.238 (5) |
| mean | 2.247 | 2.211 | 2.234 |
| *V* (Å³) | 14.40 | 13.93 | 14.26 |
| OAV | 99.43 | 75.04 | 98.45 |
| OQE | 1.0467 | 1.0255 | 1.0303 |
| M1-P3a | 2.954 (1) | 2.791 (1) | 2.849 (2) |
| M4a-P2a | 2.780 (1) | 2.741 (1) | 2.788 (1) |
| M4b-P2b | 2.758 (1) | 2.729 (1) | 2.803 (1) |
| M5a-P4a | 2.900 (1) | 2.888 (1) | 2.917 (1) |
| M5b-P4b | 2.878 (1) | 2.889 (1) | 2.924 (1) |
| W1-H1 | 0.83 | 0.80 | 0.83 |
| W2-H2 | 0.95 | 0.85 | 1.06 |
| O3x-H3x | 1.14 | 1.27 | |

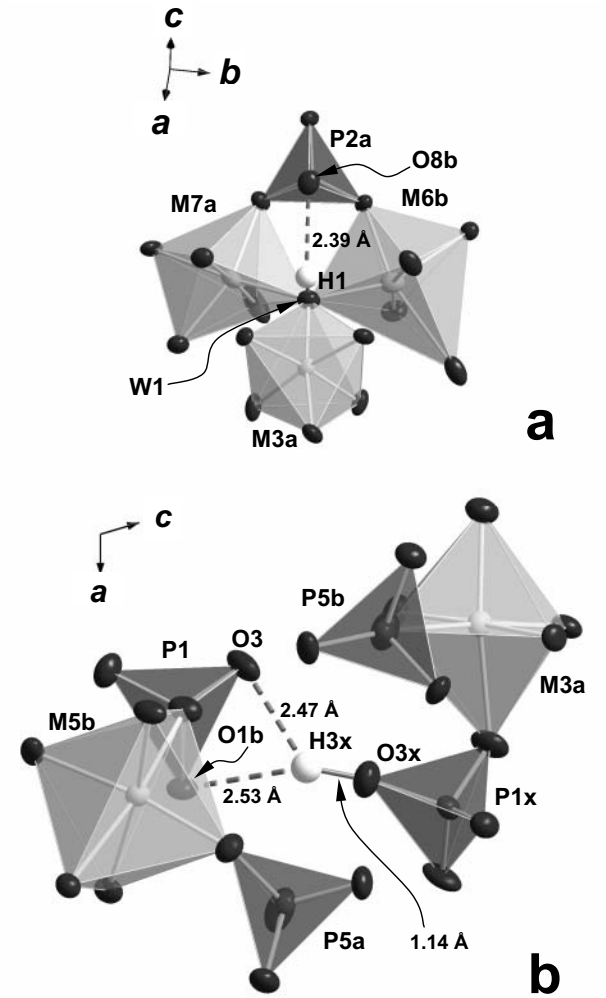


**FIGURE 4.** Sketches of the structural environments around the H atoms: (**a**) H1 (H2 is very similar); (**b**) H3x.

chemical role of the large sites suitable to incorporate large monovalent and divalent cations and excess (beyond 13 apfu) transition metals.

Generally speaking, there are eight possible sites in the arrojadite structure that are available for extra-framework cations, namely Ca, Na1, Na2, Na3, A1, A2, B1, and B2. Na3 is present in only a few samples (Branchville and the Nickel Plate Mine, in our experience), and its occupancy is sterically incompatible with that of H3x.

Three sites are always fully occupied in all the studied samples: Ca, Na1, and Na2. They are all eightfold-coordinated, and their preferred occupancy (as obtained in this work) is expressed by the selected name.

For the four remaining sites, the situation is more complex because these sites can be occupied by monovalent and divalent cations, but also may be vacant. The arrojadite samples of this work represent quite well three extreme situations, and were thus used to fix the main crystal-chemical exchanges and to build up a new nomenclature scheme based on crystal chemistry, where the suffixes are related to the predominant species at the A1, B1, and Na3 sites (cf. Part II, Chopin et al. 2006, this volume, for more detail).

In the sample from Rapid Creek, the four sites are all fully occupied by monovalent cations. Refined site-scattering values show that K is ordered at the A1 site, and hence the sample is named arrojadite-(KNa).

In the sample from Horrsjöberg, Sr and other large divalent cations are dominant at the A1 site, and charge balance is maintained by the presence of an equal amount of vacancies at the A2 site. Analogously, excess transition metals are dominant at the B1 site, and charge balance is maintained by the presence of an equal amount of vacancies at the B2 site. This sample is thus named arrojadite-(SrFe).

In the sample from Branchville, K is dominant at the A1 site, and excess transition metals are dominant at the B1 site. Moreover, the Na3 site is more than half occupied. As a consequence, this sample is named dickinsonite-(KMnNa).

Actually, the A and B sites quite often have a mixed occupancy of cations of different size, which thus have distinct local environments. Because the different local environments are averaged over the crystal by X-ray diffraction, static order is represented in the electron density map by two or more maxima occurring into the same cavity. These split sites are

**TABLE 4C.** The alkali sites: Interatomic distances (Å) and selected geometrical parameters for the arrojadites of this work

| | Rapid Cr. | Horrsjöb. | Branch. | | Rapid Cr. | Horrsjöb. | Branch. | | Rapid Cr. | Horrsjöb. | Branch. |
|---|---|---|---|---|---|---|---|---|---|---|---|
| Ca-O4 | 2.353(3) | 2.206(3) | 2.334(4) | A1-O17a | 2.902(3) | 2.850(4) | 3.088(7) | A1x-O6a | | | 2.373 (5) |
| Ca-O7a | 2.729(3) | 2.785(4) | 2.843(5) | A1-O17b | 2.820(3) | 2.764(4) | 2.920(5) | A1x-O7a | | | 2.649 (5) |
| Ca-O8a | 2.398(3) | 2.294(4) | 2.379(6) | A1-O18a | 2.695(3) | 2.644(4) | 2.799(6) | A1x-O17a | | | 2.593 (5) |
| Ca-O8b | 2.353(3) | 2.192(3) | 2.302(4) | A1-O18b | 2.745(3) | 2.684(4) | 2.883(4) | A1x-O18b | | | 2.433 (5) |
| Ca-O15a | 2.396(2) | 2.211(4) | 2.332(4) | A1-O21a | 3.091(3) | 2.875(4) | 3.043(7) | A1x-O21a | | | 2.770 (5) |
| Ca-O15b | 2.744(3) | 3.003(4) | 2.855(4) | A1-O21b | 3.110(3) | 2.853(4) | 2.913(5) | A1x-O22b | | | 2.711 (5) |
| Ca-O16a | 2.483(3) | 2.554(4) | 2.507(5) | A1-O22a | 2.859(3) | 2.731(4) | 2.892(7) | mean | | | 2.588 |
| Ca-O16b | 2.320(3) | 2.163(3) | 2.250(4) | A1-O22b | 2.814(3) | 2.805(4) | 2.912(4) | $V$ (Å$^3$) | | | 15.00 |
| mean | 2.472 | 2.426 | 2.475 | mean | 2.879 | 2.776 | 2.931 | | | | |
| $V$ (Å$^3$) | 25.83 | 24.14 | 25.69 | $V$ (Å$^3$) | 33.67 | 30.12 | 34.50 | | | | |
| A2-O1b | 2.576(4) | | 2.686(5) | A2x-O1a | 2.613(3) | | 2.746(5) | B1-O2a | 2.420(3) | 2.458(7) | 2.519 (6) |
| A2-O3 | 2.354(3) | | 2.395(7) | A2x-O1b | 3.047(3) | | 3.131(5) | B1-O4x | 3.229(3) | 3.207(8) | 3.043 (5) |
| A2-O3x | 2.412(3) | | 2.362(10) | A2x-O3 | 2.006(3) | | 2.708(5) | B1-O8a | 2.189(3) | 2.116(9) | 2.209 (6) |
| A2-O21a | 2.597(4) | | 2.769(7) | A2x-O3x | 2.597(3) | | 1.640(8) | B1-O10a | 3.206(3) | 3.275(8) | 3.243 (6) |
| A2-O22b | 2.978(4) | | 2.818(8) | A2x-O4x | 2.736(3) | | 3.026(5) | B1-O11b | 2.349(3) | 2.333(8) | 2.383 (4) |
| A2-O23a | 2.479(4) | | 3.049(7) | A2x-O21b | 2.759(4) | | 3.172(6) | B1-O12a | 2.345(3) | 2.513(7) | 2.405 (6) |
| A2-O23b | 2.948(4) | | 3.085(6) | A2x-O23a | 2.798(3) | | 3.141(5) | B1-O12b | 3.303(3) | 3.244(8) | 3.260 (5) |
| mean$^{VII}$ | 2.621 | | 2.738 | A2x-O23b | 2.926 | | 2.868(5) | B1-O15b | 3.334(3) | 3.070(8) | 3.294 (4) |
| $V$ (Å$^3$) | 21.62 | | 18.92 | mean $^{IV}$ | | | 2.490 | mean$^{IV}$ | 2.326 | 2.355 | 2.379 |
| | | | | mean $^{VIII}$ | 2.685 | | 2.804 | mean$^{VIII}$ | 2.797 | 2.777 | 2.795 |
| | | | | $V$ (Å$^3$) $^{VIII}$ | 26.54 | | 25.74 | V$^{IV}$ (Å$^3$) $^{IV}$ | 4.42 | 4.51 | 4.65 |
| B1x-O2a | | 2.588(5) | | B1y-O2a | | 2.751(5) | | B2-O5b | 2.937(3) | 3.015(6) | 2.964 (5) |
| B1x-O4x | | 2.578(5) | | B1y-O4x | | 2.553(7) | | B2-O10a | 2.348(3) | 2.351(5) | 2.336 (6) |
| B1x-O8a | | 2.439(6) | | B1y-O8a | | 2.627(6) | | B2-O13a | 2.288(3) | 2.223(5) | 2.308 (5) |
| B1x-O10a | | 2.556(4) | | B1y-O10a | | 2.380(6) | | B2-O16a | 3.026(3) | 2.816(6) | 2.992 (6) |
| B1x-O12a | | 2.433(4) | | B1y-O12a | | 2.474(7) | | B2-O17b | 2.467(3) | 2.610(6) | 2.577 (4) |
| B1x-O16a | | 2.564(5) | | B1y-O16a | | 2.453(7) | | B2-O20b | 2.485(3) | 2.427(6) | 2.406 (4) |
| B1x-O24b | | 3.003(6) | | B1y-O24b | | 2.751(7) | | B2-O21b | 2.404(3) | 2.441(6) | 2.427 (5) |
| mean$^{VI}$ | | 2.595 | | mean$^{VII}$ | | 2.570 | | B2-O24b | 2.367(3) | 2.306(6) | 2.458 (4) |
| $V$ (Å$^3$) | | 23.00 | | $V$ (Å$^3$) | | 23.00 | | mean | 2.540 | 2.524 | 2.558 |
| | | | | | | | | $V$ (Å$^3$) | 25.39 | 25.37 | 26.42 |
| | | | | | | | | | Branch. | | Branch. |
| Na1-O9a | 2.524(4) | 2.634(4) | 2.548(6) | Na2-O5a | 3.031(4) | 3.105(4) | 3.165(7) | Na3-O2b | 2.496(5) | Na3x-O2a | 2.430 (4) |
| Na1-O9b | 2.601(4) | 2.624(4) | 2.596(5) | Na2-O10b | 2.354(4) | 2.323(4) | 2.343(4) | Na3-O3x | 2.075(12) | Na3x-O3x | 1.446(11) |
| Na1-O11a | 2.981(4) | 2.659(4) | 2.807(7) | Na2-O13b | 2.375(4) | 2.365(4) | 2.384(5) | Na3-O17a | 2.483(8) | Na3x-O17a | 3.120 (5) |
| Na1-O11b | 2.632(4) | 2.571(4) | 2.680(5) | Na2-O16b | 2.714(4) | 2.689(4) | 2.709(6) | Na3-O17b | 2.970(6) | Na3x-O17b | 2.682 (5) |
| Na1-O14a | 2.353(4) | 2.424(4) | 2.379(6) | Na2-O17a | 2.502(4) | 2.696(5) | 2.838(8) | Na3-O18a | 2.735(8) | Na3x-O18a | 2.509 (5) |
| Na1-O14b | 2.318(4) | 2.381(4) | 2.352(4) | Na2-O20a | 2.499(4) | 2.384(4) | 2.365(6) | Na3-O18b | 2.419(6) | Na3x-O18b | 3.006 (5) |
| Na1-O15a | 2.507(4) | 2.453(4) | 2.527(7) | Na2-O21a | 2.605(4) | 2.551(5) | 2.660(9) | Na3-O19a | 2.954(8) | Na3x-O19a | 2.969 (6) |
| Na1-O15b | 2.588(4) | 2.503(4) | 2.625(5) | Na2-O24a | 2.385(4) | 2.418(4) | 2.406(6) | Na3-O19b | 2.808(6) | Na3x-O19b | 2.768 (6) |
| mean | 2.563 | 2.531 | 2.564 | mean | 2.558 | 2.571 | 2.609 | mean $^{IV}$ | 2.368 | mean $^{IV}$ | 2.267 |
| $V$ (Å$^3$) | 25.83 | 24.67 | 25.66 | $V$ (Å$^3$) | 25.42 | 25.51 | 27.04 | mean $^{VIII}$ | 2.617 | mean $^{VIII}$ | 2.616 |
| | | | | | | | | V$^{VIII}$ (Å$^3$) | 26.32 | V$^{VIII}$ (Å$^3$) | 22.58 |

indicated by x and y in Table 4.

This feature can be used to detect the main solid solution mechanisms and exchange vectors. Figure 5 shows the relevant Fourier maps ($2F_o - F_c$) obtained at convergence for the three samples of this work. In the sample from Rapid Creek, the electron density at the A2 site is clearly split into two maxima (A2 and A2x), the weaker of which has peak electron density values slightly higher than that corresponding to the H3x site; in this sample, there is no evidence of cations occurring at the Na3 site. In the sample from Horrsjöberg, there is no electron density either at the A2 site or at the Na3 sites, whereas the maximum related to the H3x site is clearly visible. In the sample from Branchville, the maxima related to the A2 and Na3 sites are well characterized, and both show distinct split positions for distinct cations; the shape of the electron density at the O3x site is oblate, and represents the superposition of distinct local situations depending on this complex cation ordering. Given the significant Na3-Na3x occupancy, the electron density at the H3x site is hardly detectable.

Although it is a clear indication of a mixed site population and it may suggest the nature of the dominant cation, the presence of split sites in some cases can make the estimation of their site scattering difficult. In fact, the refined model adopts either isotropic or anisotropic atomic displacement factors, which may not represent all the experimental electron density. Calculation of accurate site populations is thus possible in arrojadite only when there is good agreement between the refined site scattering and the values calculated from the unit formula, and must rely

**TABLE 4D.** Alkali sites—intercationic distances: Interatomic distances (Å) and selected geometrical parameters for the arrojadites of this work

| | Rapid Creek | Horrsjöberg | Branchville |
|---|---|---|---|
| Ca-P4a | 3.004(1) | 2.927 (1) | 2.975(1) |
| A1-A1x | | | 1.634(7) |
| A2-A2x | 1.071(2) | | 0.847(5) |
| B1-B1x | | 1.285 (7) | |
| B1-B1y | | 1.644(12) | |
| B1x-B1y | | 0.365(12) | |
| B2-P4a | 3.121(2) | 2.984 (5) | 3.130(4) |
| B2-P6b | 2.911(2) | 2.847 (4) | 2.943(4) |
| B2-B1 | 3.971(2) | | 3.867(7) |
| B2-B1x | | 2.593 (7) | |
| B2-B1y | | 2.230 (9) | |
| Na3-Na3x | | | 1.003(5) |
| Na1-P4a | 2.943(2) | 2.947 (2) | 2.973(5) |
| Na1-P4b | 2.938(2) | 2.925 (2) | 2.983(4) |

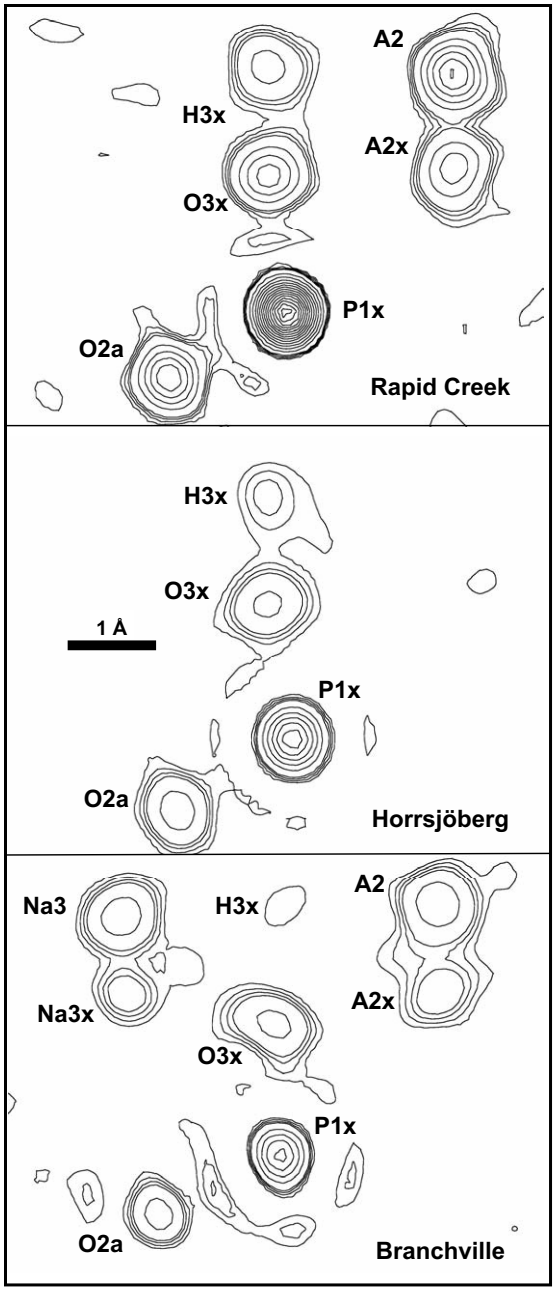


**FIGURE 5.** Electron density maps ($2F_o - F_c$) projected onto the plane containing the O3x, H3x, A2, and Na3 sites, ($10\bar{1}$). Contours are drawn at 2, 3, 4, 5, 10, 15, 20…. e/Å$^3$.

also on the refined bond lengths. Given the complexity of the chemistry and of the structure, it is reasonable to report only on the site preference of the various cations. Therefore, the electron density maps in Figure 5 show that (1) the total occupancy of the A2 and Na3 can vary from 0 to 1 apfu; (2) the occupancy of H3x is inversely related to that of the Na3 site; and (3) both the Na3 and A2 sites can be occupied by larger (monovalent) and smaller (divalent) cations, the amounts of which can be roughly estimated based on all the crystal-chemical details available.

## Perspective

We have now established the correct structure, stoichiometry, and the crystal-chemical relations between the sites occupied by the large cations. As a next step (Part II, Chopin et al. 2006, this volume), we extend this study to other samples covering a range of compositions and we define a rational scheme for the arrojadite-group nomenclature, which rests on crystal chemistry but can be used without the need of structure refinement.

## ACKNOWLEDGMENTS

Thanks are due to Massimo Tiepolo for LA-ICP-MS analysis. This work was partly funded by the MIUR-PRIN 2005 project "From minerals to materials: crystal-chemistry, microstructures, modularity, modulations".

## REFERENCES CITED

Brown, I.D. and Altermatt, D. (1985) Bond-valence parameters obtained from a systematic analysis of the Inorganic Crystal Structure Database. Acta Crystallographica, B41, 244–247.

Brush, G.J. and Dana, E.S. (1878) On a new and remarkable mineral locality in Fairfield County, Connecticut; with a description of several new species occurring there. American Journal of Science, 16, 33–46; 114–123.

Brush, G.J., Dana, E.S., and Wells, H.L. (1890) On the mineral locality at Branchville, Connecticut: fifth paper; with analyses of several manganesian phosphates. American Journal of Science, 39, 201–216.

Busing, W.R., Martin, K.O., and Levy, H.A. (1962) Report ORNL-TM-305, 75 p. Oak Ridge National Laboratory, Tennessee.

Chopin, C., Oberti, R., and Cámara, F. (2006) The arrojadite enigma: II. Compositional space, new members and nomenclature of the group. American Mineralogist, 91, 1260–1270.

Demartin, F., Gramaccioli, C.M., Pilati, T., and Sciesa, E. (1996) Sigismundite, $(Ba,K,Pb)Na_3(Ca,Sr)(Fe,Mg,Mn)_{14}(OH)_2(PO_4)_{12}$, a new Ba-rich member of the arrojadite group from Spluga valley, Italy. Canadian Mineralogist, 34, 827–834.

Ek, R. and Nysten, P. (1990) Phosphate mineralogy of the Hålsjöberg and Hökensås kyanite deposits. Geologiska Föreningens i Stockholm Förhandlingar, 112, 9–18.

Fleischer, M., Wilcox, R.E., and Matzko, J.J. (1985) Microscopic determination of the nonopaque minerals. USGS Bulletin 1627.

Henriques, A. (1956) An iron-rich wagnerite, formerly named talktriplite, from Hållsjöberget (Horrsjöberget), Sweden. Arkiv för Mineralogi och Geologi, 2(6), 149–153.

Huminicki, D.M.C. and Hawthorne, F.C. (2002) The crystal chemistry of the phosphate minerals. In M.L. Kohn, J. Rakovan, and J.M. Hughes, Eds., Phosphates: geochemical, geobiological, and materials importance, 48, 123–254. Reviews in Mineralogy and Geochemistry, Mineralogical Society of America, Chantilly, Virginia.

Jaulmes, S., Elfakir, A., Quarton, M., Brunet, F., and Chopin, C. (1997) Structure cristalline de la phase haute température et haute pression de $Mg_3(PO_4)_2$. Journal of Solid State Chemistry, 129, 341–345.

Krutik, V.M., Pushcharovskii, D.Yu., Pobedimskaya, E.A., and Belov, N.V. (1979) Crystal structure of arrojadite. Kristallografiya, 24, 743–750.

Merlino, S., Mellini, M., and Zanazzi, P.F. (1981) Structure of arrojadite, $KNa_4CaMn_4Fe_{10}Al(PO_4)_{12}(OH,F)_2$. Acta Crystallographica, B37, 1733–1736.

Moore, P.B., Araki, T., Merlino, S., Mellini, M., and Zanazzi, P.F. (1981) The arrojadite-dickinsonite series, $KNa_4Ca(Fe,Mn^{2+})_{14}Al(OH)_2(PO_4)_{12}$: crystal structure and crystal chemistry. American Mineralogist, 66, 1034–1049.

Robinson, G.W., van Velthuizen, J., Ansell, H.G., and Sturman, B.D. (1992) Mineralogy of the Rapid Creek and Big Fish River area, Yukon Territory. Mineralogical Record, 23, 1–47.

Shainin, V.E. (1946) The Branchville, Connecticut, pegmatite. American Mineralogist, 31, 329–345.

Steele, I.M. (2002) Arrojadite: variations in space group and composition based on four new refinements. 18th IMA General Meeting, Edinburgh, Abstracts, MO2-117.

Stormer, J.C., Pierson, M.L., and Tacker, R.C. (1993) Variation of F and Cl X-ray intensity due to anisotropic diffusion in apatite during electron microprobe analysis. American Mineralogist, 78, 641–648.

van Achterbergh, E., Ryan, C.G., Jackson, S.E., and Griffin, W.L. (2001) Data reduction software for LA-ICP-Ms. In P.J. Sylvester, Ed., Laser Ablation ICPMS in the Earth Sciences: Principles and Applications, 29, 239–243. Mineralogical Association of Canada, Short Course Series, Ottawa.

Yakubovich, O.V., Matviyenko, Ye.N., Simonov, M.A., and Mel'nikov, O.K. (1986) The crystalline structure of synthetic $Fe^{3+}$-arrojadites with the idealized formula $K_2Na_5Fe^{2+}_{14}Fe^{3+}(PO_4)_{12}(OH)_2$. Vestnik Moskovovskogo Universiteta, Seriya Geologiya, 1986, 36–47.

MANUSCRIPT RECEIVED DECEMBER 13, 2005
MANUSCRIPT ACCEPTED MARCH 28, 2006
MANUSCRIPT HANDLED BY PAOLA BONAZZI

## APPENDIX. FURTHER MINERAL DATA FOR THE TWO NEW END-MEMBERS OF THE ARROJADITE GROUP

The specimens investigated in this paper have been recognized as the holotype material of three members of the arrojadite group. As requested by the IMA procedure, we report hereafter their complete mineral description.

In particular, given the uncertainty on the exact composition of the Serra Branca material (for which the arrojadite name has first been proposed, see Part II, Chopin et al. 2006, this volume) and the nearly stoichiometric end-member composition of the sample from Rapid Creek (ENSMP no. 41081), the latter has been recognized by IMA-CNMMN as the new holotype of arrojadite-(KNa) (vote 2005-047). The sample from Horrsjöberg (ENSMP no. 16926) is the holotype material for arrojadite-(SrFe) (vote 2005-032), and the sample from Branchville (ENSMP no. 4861) is the holotype material for dickinsonite-(KMnNa) (vote 2005-048). All these samples are part of the collection of the Musée de Minéralogie, Ecole des Mines de Paris.

### CHEMISTRY

The ideal end-member composition for arrojadite-(KNa), $^{A1}K\,^{A2}Na\,^{B1}Na\,^{B2}Na\,^{Na1,2}Na_2\,^{Na3}\square\,^{Ca}Ca\,^{M}Fe_{13}\,Al\,(PO_4)_{11}\,^{P1x}(PO_3OH_1)\,^{W}(OH)_2$, would correspond to: $P_2O_5$ = 40.14, $Al_2O_3$ = 2.40, FeO = 44.02, CaO = 2.64, $Na_2O$ = 7.31, $K_2O$ = 2.22, and $H_2O$ = 1.27 wt%.

The ideal end-member composition for arrojadite-(SrFe), $^{A1}Sr\,^{A2}\square\,^{B1}Fe^{2+}\,^{B2}\square\,^{Na1,2}Na_2\,^{Na3}\square\,^{Ca}Ca\,^{M}Fe^{2+}_{13}Al(PO_4)_{11}\,^{P1x}(PO_3OH)\,^{W}(OH)_2$, would correspond to: $P_2O_5$ = 39.48, $Al_2O_3$ = 2.36, FeO = 46.63, CaO = 2.60, $Na_2O$ = 2.87, SrO = 4.80, and $H_2O$ = 1.25 wt%.

The ideal end-member composition of dickinsonite-(KMnNa), $^{A1}K\,^{A2}Na\,^{B1}Mn\,^{B2}\square\,^{Na1,2}Na_2\,^{Na3}Na\,^{Ca}Ca\,^{M}(Mn,Fe,Mg)_{13}\,Al\,(PO_4)_{11}\,^{P1x}(PO_4)\,^{W}(OH)_2$, would correspond to: $P_2O_5$ 39.78, $Al_2O_3$ 2.38, MnO 46.39, CaO 2.62, $Na_2O$ 5.79, $K_2O$ 2.20, $H_2O$ 0.84 wt%.

### OCCURRENCE AND PARAGENESIS

**Arrojadite-(KNa).** The mineral occurs as coating of open fractures in siderite-rich Lower Cretaceous sandstones of the Rapid Creek area, northwestern Yukon Territory, Canada, a locality famous for the number and quality of rare phosphate minerals found there (Robinson et al. 1992). The sample studied is preserved in the collections of the Musée de Minéralogie, Ecole des Mines de Paris (ENSMP), under reference no. 41081 since 1980. Associated minerals include euhedral quartz and some limonite (former siderite?). Arrojadite-(KNa) (and quartz) represent the early stage of phosphate mineral precipitation in veins, which occurred from low-salinity fluids during or after the Laramide orogeny, under very low-grade metamorphic conditions, at minimum temperatures of 180–200 °C (Robinson et al. 1992).

**Arrojadite-(SrFe).** The mineral occurs as a common rock-forming mineral in a fist-size sample of kyanite-muscovite-wagnerite-lazulite rock from the Horrsjöberg locality in Värmland, Sweden. The locality (also spelt Hållsjöberg, Hålsjöberg, etc.) is famous for the kyanite-quartzite hosting a variety of Al-phosphates (e.g., berlinite, trolleite, svanbergite; see, e.g., Ek and Nysten 1990). Associated minerals include fine-grained kyanite that forms the groundmass of the sample, spotted by conspicuous orange-brown wagnerite crystals ("talktriplit," "magniotriplit," cf. Henriques 1956), and dark-blue patches consisting of abundant interstitial lazulite that commonly overgrows arrojadite-(SrFe), and a wyllieite-group mineral. Muscovite, rutile, hematite (in part secondary, with lazulite), and quartz are other minor constituents, as well as accessory fluorapatite (cf. Ek and Nysten 1990). The mineral assemblage is reminiscent of the "stratabound thin intercalations in the quartzite" reported by Ek and Nysten (1990) that represent the earliest phosphate paragenesis. Arrojadite-(SrFe) belongs to the early paragenesis (together with kyanite, muscovite, rutile, wagnerite, and wyllieite), which formed by either hydrolyzing solutions during Precambrian amphibolite-facies (500–575 °C, >3 kbar) metamorphism of argillaceous sediments (and volcanics?), or by amphibolite-facies metamorphism of an Al-rich, phosphate-bearing residual rock after alteration of supracrustal rocks in a hot-spring environment (Ek and Nysten 1990).

**Dickinsonite-(KMnNa).** The mineral occurs as green polycrystalline masses in the pegmatite at Branchville, Fairfield Co., Connecticut (e.g., Shainin 1946), which is a classic locality for Mn-phosphates and the type-locality of nine species, including dickinsonite (Brush and Dana 1878; Brush et al. 1890). According to these authors, dickinsonite is associated intimately with eosphorite, triploidite, lithiophilite, and other species in nests in a vein of albitic granite, most likely in the "cleavelandite"-spodumene unit of the pegmatite (Shainin 1946). In the Branchville dickinsonite sample studied (ENSMP no. 4861), green cm-sized nodular masses in albitic granite consist only of dickinsonite lamellae intergrown with quartz.

#### Physical and optical properties

Arrojadite-(KNa) is found as clear, yellow, mm-sized euhedral crystals. Stout, more-or-less platy prisms have (001) cleavage, possibly less good than in other members of the group.

Arrojadite-(SrFe) could only be observed in petrographic thin sections. It forms isolated, slightly elongated crystals, originally up to several hundred μm in the longest dimension, now invariably corroded and rimmed by lazulite, hematite, and minor fluorapatite. This alteration pattern is almost a diagnostic feature.

Dickinsonite-(KMnNa) is found as mica-like platelets with a vivid green color, typically a few hundred μm in size, intimately intergrown with quartz.

Mohs hardness was not measured, but should be around 3.5 to 4 (Brush and Dana 1878). The streak is white and the luster is vitreous for all the samples. Arrojadites are non-fluorescent. The calculated density is 3.437 g/cm$^3$ for arrojadite-(KNa), 3.569 g/cm$^3$ for arrojadite-(SrFe), and 3.496 g/cm$^3$ for dickinsonite-(KMnNa).

Arrojadite-(KNa) is biaxial (+), with $n_\alpha$ = 1.651(1), $n_\beta$ = 1.656(1), $n_\gamma$ = 1.662(10) (589 nm). 2V (meas.) = 87.8(1)° (direct measurement); 2V (calc.) = 85°. Dispersion: r << v. Orientation, checked by X-ray diffraction: X = b; Y ≈ c. Pleochroism: very

weak, Y colorless < X ≈ Z pale yellow.

Arrojadite-(SrFe) is biaxial (+), with $n_\alpha$ = 1.654(1), $n_\beta$ = 1.657(2), $n_\gamma$ = 1.668(1) (589 nm). 2V (meas.) was 41(1) and 37(2)° for two measured crystals (from spindle-stage extinction curves); 2V (calc.) = 55° (possible range 34–69°). Pleochroism: very weak, X ≈ Y colorless, Z pale yellow.

Dickinsonite-(KMnNa) is biaxial (+), with $n_\alpha$ = 1.658, $n_\beta$ = 1.662, $n_\gamma$ = 1.671 (589 nm) with X = *b* and Y ∧ c = 15°. 2V (calc.) = 68°. Dispersion: r >> v. Pleochroism: very weak, X pale olive green > Y paler olive green > Z very pale yellow green (all data from Fleischer et al. 1985).

## X-RAY POWDER DIFFRACTION

Due to the common presence of alteration and inclusions, powder X-ray (Cu*K*α radiation) diffraction data were calculated for all the samples from single-crystal data; the most intense reflections are tabulated in Table A1 for recognition purposes.

**TABLE A1.** X-ray powder diffraction data calculated from single-crystal data

| *h* | *k* | *l* | 2θ$_{calc}$ | *d*$_{calc}$ | *I*/*I*$_0$ | *h* | *k* | *l* | 2θ$_{calc}$ | *d*$_{calc}$ | *I*/*I*$_0$ | *h* | *k* | *l* | 2θ$_{calc}$ | *d*$_{calc}$ | *I*/*I*$_0$ | *h* | *k* | *l* | 2θ$_{calc}$ | *d*$_{calc}$ | *I*/*I*$_0$ |
|---|---|---|---|---|---|---|---|---|---|---|---|---|---|---|---|---|---|---|---|---|---|---|---|
| **(a) arrojadite-(KNa)** | | | | | | | | | | | | | | | | | | | | | | | |
| 2 | 0 | 2 | 11.53 | 7.6734 | 13.8 | $\bar{1}$ | 3 | 2 | 27.81 | 3.2082 | 22.1 | **$\bar{5}$** | **1** | **6** | **32.04** | **2.7933** | **28.0** | 0 | 4 | 0 | 35.73 | 2.5132 | 18.5 |
| 1 | 1 | 2 | 13.74 | 6.4470 | 16.9 | **2** | **0** | **6** | **28.01** | **3.1857** | **33.5** | **4** | **0** | **8** | **32.23** | **2.7774** | **24.4** | 4 | 2 | 8 | 36.98 | 2.4309 | 14.7 |
| 0 | 0 | 4 | 15.00 | 5.9079 | 14.3 | **4** | **2** | **4** | **29.28** | **3.0498** | **100.0** | 3 | 3 | 1 | 32.42 | 2.7615 | 12.5 | 6 | 2 | 2 | 37.24 | 2.4147 | 13.3 |
| **2** | **0** | **2** | **15.11** | **5.8614** | **28.8** | **5** | **1** | **4** | **29.28** | **3.0498** | | **6** | **0** | **2** | **32.52** | **2.7532** | **22.8** | 7 | 1 | 6 | 40.89 | 2.2072 | 8.6 |
| 2 | 0 | 4 | 15.95 | 5.5547 | 12.5 | **3** | **3** | **2** | **31.35** | **2.8529** | **22.4** | 3 | 1 | 6 | 33.20 | 2.6981 | 21.5 | 8 | 0 | 8 | 47.39 | 1.9183 | 9.0 |
| **0** | **2** | **0** | **17.64** | **5.0264** | **27.5** | **3** | 1 | 8 | 31.48 | 2.8414 | 16.4 | **2** | **2** | **6** | **33.30** | **2.6908** | **71.3** | 2 | 4 | 10 | 51.97 | 1.7596 | 9.7 |
| 1 | 1 | 4 | 19.53 | 4.5371 | 9.1 | 3 | 3 | 0 | 31.61 | 2.8308 | 13.4 | 1 | 3 | 6 | 34.55 | 2.5959 | 9.8 | 2 | 0 | 14 | 52.09 | 1.7557 | 9.4 |
| 1 | 1 | 6 | 26.35 | 3.3821 | 19.3 | 0 | 2 | 7 | 31.93 | 2.8085 | 14.8 | 0 | 2 | 8 | 35.24 | 2.5467 | 11.1 | 6 | 4 | 2 | 52.28 | 1.7498 | 8.9 |
| 3 | 1 | 4 | 27.11 | 3.2886 | 14.6 | **1** | **3** | **4** | **31.99** | **2.7979** | **24.9** | 4 | 2 | 4 | 35.45 | 2.5318 | 19.3 | 8 | 2 | 4 | 56.00 | 1.6421 | 9.4 |
| **(b) arrojadite-(SrFe)** | | | | | | | | | | | | | | | | | | | | | | | |
| 2 | 0 | 2 | 15.08 | 5.8759 | 17.6 | $\bar{1}$ | 3 | 2 | 28.14 | 3.1713 | 13.9 | **$\bar{6}$** | **0** | **2** | **32.80** | **2.7304** | **20.1** | $\bar{6}$ | 2 | 4 | 38.07 | 2.3634 | 9.6 |
| 0 | 2 | 0 | 17.85 | 4.9700 | 14.9 | **4** | **2** | **4** | **29.69** | **3.0093** | **100.0** | **2** | **2** | **6** | **33.36** | **2.6861** | **69.9** | 7 | 1 | 6 | 41.47 | 2.1773 | 10.6 |
| 3 | 1 | 2 | 18.77 | 4.7268 | 9.1 | **3** | **3** | **2** | **31.73** | **2.8202** | **23.5** | **3** | **3** | **4** | **33.37** | **2.6847** | | 8 | 0 | 8 | 48.13 | 1.8906 | 9.8 |
| 0 | 2 | 2 | 19.38 | 4.5790 | 17.2 | **3** | **1** | **8** | **31.90** | **2.8053** | **28.4** | 3 | 3 | 2 | 33.89 | 2.6449 | 8.8 | 6 | 4 | 2 | 52.62 | 1.7394 | 10.9 |
| 1 | 1 | 4 | 19.59 | 4.5314 | 19.1 | **3** | **3** | **0** | **31.91** | **2.8047** | | 1 | 3 | 6 | 34.91 | 2.5703 | 10.9 | 1 | 5 | 6 | 52.62 | 1.7394 | |
| 2 | 2 | 2 | 21.39 | 4.1533 | 10.6 | 1 | 3 | 4 | 32.23 | 2.7770 | 10.3 | 0 | 2 | 8 | 35.43 | 2.5332 | 11.2 | 8 | 2 | 4 | 56.05 | 1.6407 | 9.4 |
| **1** | **1** | **6** | **26.38** | **3.3784** | **26.2** | 5 | 1 | 6 | 32.54 | 2.7518 | 12.2 | **4** | **2** | **4** | **35.49** | **2.5291** | **23.1** | 0 | 6 | 2 | 56.06 | 1.6405 | |
| **3** | **1** | **4** | **27.08** | **3.2931** | **21.0** | **4** | **0** | **8** | **32.72** | **2.7370** | **27.8** | 0 | 4 | 0 | 36.15 | 2.4850 | 18.4 | | | | | | |
| **2** | **0** | **6** | **27.95** | **3.1925** | **41.2** | **3** | **3** | **1** | **32.69** | **2.7396** | | 6 | 2 | 2 | 37.58 | 2.3931 | 11.7 | | | | | | |
| **(c) dickinsonite-(KMnNa)** | | | | | | | | | | | | | | | | | | | | | | | |
| 2 | 0 | 2 | 11.49 | 7.7017 | 20.3 | $\bar{1}$ | 3 | 2 | 27.67 | 3.2233 | 17.9 | **$\bar{6}$** | **0** | **2** | **32.22** | **2.7785** | **28.6** | $\bar{6}$ | 2 | 2 | 36.92 | 2.4345 | 18.9 |
| 1 | 1 | 2 | 13.56 | 6.5321 | 17.4 | **5** | **1** | **4** | **29.14** | **3.0646** | **100.0** | 3 | 1 | 6 | 32.60 | 2.7469 | 9.0 | 7 | 1 | 6 | 40.70 | 2.2170 | 9.6 |
| **0** | **0** | **4** | **14.79** | **5.9892** | **21.0** | **4** | **2** | **4** | **29.16** | **3.0623** | | **3** | **3** | **4** | **32.80** | **2.7304** | **89.1** | 8 | 0 | 8 | 47.20 | 1.9254 | 8.6 |
| **2** | **0** | **2** | **14.83** | **5.9715** | **26.8** | 3 | **3** | **2** | **31.19** | **2.8675** | **26.6** | **2** | **2** | **6** | **32.81** | **2.7299** | | 2 | 0 | 14 | 51.52 | 1.7738 | 9.9 |
| 2 | 0 | 4 | 15.90 | 5.5749 | 13.6 | 3 | 1 | 8 | 31.32 | 2.8561 | 16.0 | 0 | 2 | 8 | 34.83 | 2.5759 | 19.4 | 2 | 4 | 10 | 51.58 | 1.7717 | 14.0 |
| **0** | **2** | **0** | **17.56** | **5.0507** | **21.5** | 3 | 3 | 0 | 31.38 | 2.8509 | 13.2 | **4** | **2** | **4** | **34.91** | **2.5702** | **27.0** | 6 | 4 | 2 | 51.70 | 1.7681 | 13.4 |
| 1 | 1 | 4 | 19.27 | 4.6047 | 10.9 | 1 | 3 | 4 | 31.70 | 2.8223 | 10.7 | 6 | 0 | 6 | 34.95 | 2.5672 | 19.1 | 8 | 2 | 4 | 55.06 | 1.6678 | 12.7 |
| 1 | 1 | 6 | 25.94 | 3.4343 | 17.2 | 5 | 1 | 6 | 31.94 | 2.8023 | 20.8 | 0 | 4 | 0 | 35.55 | 2.5253 | 18.7 | 0 | 6 | 2 | 55.08 | 1.6672 | 11.4 |
| **2** | **0** | **6** | **27.49** | **3.2447** | **32.7** | **4** | **0** | **8** | **32.11** | **2.7875** | **26.6** | 4 | 2 | 8 | 36.83 | 2.4405 | 19.5 | 1 | 3 | 12 | 55.08 | 1.6672 | |

*Note:* The 10 strongest reflections are shown in bold.